



Experimental study of high pressure phase equilibrium of (CO₂ + NO₂/N₂O₄) mixtures

Séverine Camy, Jean-jacques Letourneau, Jean-Stéphane Condoret

► To cite this version:

Séverine Camy, Jean-jacques Letourneau, Jean-Stéphane Condoret. Experimental study of high pressure phase equilibrium of (CO₂ + NO₂/N₂O₄) mixtures. *Journal of Chemical Thermodynamics*, 2011, 43 (12), pp.1954-1960. 10.1016/j.jct.2011.07.007 . hal-01668418

HAL Id: hal-01668418

<https://hal.science/hal-01668418>

Submitted on 22 Mar 2019

HAL is a multi-disciplinary open access archive for the deposit and dissemination of scientific research documents, whether they are published or not. The documents may come from teaching and research institutions in France or abroad, or from public or private research centers.

L'archive ouverte pluridisciplinaire **HAL**, est destinée au dépôt et à la diffusion de documents scientifiques de niveau recherche, publiés ou non, émanant des établissements d'enseignement et de recherche français ou étrangers, des laboratoires publics ou privés.

Experimental study of high pressure phase equilibrium of (CO₂ + NO₂/N₂O₄) mixtures

S. Camy^{a,b,*}, J.-J. Letourneau^c, J.-S. Condoret^{a,b}

^a Université de Toulouse, INPT, UPS, Laboratoire de Génie Chimique, 4, Allée Emile Monso, F-31030 Toulouse, France

^b CNRS, Laboratoire de Génie Chimique, F-31030 Toulouse, France

^c Université de Toulouse, Mines Albi, CNRS, Centre RAPSODEE, F-81013 Albi cedex 09, France

A B S T R A C T

Experimental bubble pressure, as well as liquid density of (CO₂ + NO₂/N₂O₄) mixtures are reported at temperatures ranging from (298 to 328.45) K. Experiments were carried out using a SITEC high-pressure variable volume cell. Transition pressures were obtained by the synthetic method and liquid density was deduced from measurement of the cell volume. Correlation of experimental results was carried out without considering chemical equilibrium of NO₂/N₂O₄ system. (Liquid + vapour) equilibrium was found to be accurately modelled using the Peng–Robinson equation of state with classical quadratic mixing rules and with a binary interaction coefficient k_{ij} equal to zero. Nevertheless, modelling of liquid density values was unsatisfactory with this approach.

Keywords:

Experimental data

Peng–Robinson equation of state

Carbon dioxide

Nitrogen dioxide

1. Introduction

Supercritical carbon dioxide is now commonly recognized as a very promising compound to be used as a green solvent for chemical reactions as replacement for polluting organic solvents. This is due not only to the interesting physical properties of supercritical compounds, but also to the chemical inertness, low cost, non-toxicity of CO₂ and the fact that this compound can be easily recycled. Although a weak solvent for polar interest molecules, scCO₂ has been used as a solvent in a wide range of chemical reactions such as hydrogenations, hydroformylations, oxidations, or polymerizations. The use of scCO₂ for chemical synthesis has been extensively reviewed by Beckman [1]. Because it is completely miscible with gases such as O₂, CO, or H₂, high pressure CO₂ is very useful to enhance solubility of reactants into liquid phases or even to alleviate liquid–gas mass transfer limitations by solubilizing all the reactants to give a single-phase system. Moreover, carbon dioxide being the result of complete oxidation of organic compounds, it cannot be oxidized, and thus it is the ideal solvent for oxidation reactions. For this reason, CO₂ has often been used as a solvent for oxidation reactions, employing mainly oxygen as the oxidant. Recently, another example of oxidation reaction in high pressure CO₂, in which nitrogen dioxide is the oxidant, has been described [2] and the process of oxidation patented [3]. This involves oxidation of polysaccharides, and more

specifically cellulose, resulting in oxidized cellulose, a very attractive material for bio-medical applications. Indeed, when cellulose is partially oxidized it becomes degradable in the human body (a property termed “bioresorbability”) and in addition possesses haemostatic properties (*i.e.* it halts bleeding), which can be advantageous in biomedical devices, like surgical compresses for instance. The suitable oxidant for preparing this material with both high carboxyl content and targeted physical properties is nitrogen dioxide (NO₂). This compound ensures selective oxidation of the primary hydroxyl groups of cellulose, leading to partially oxidized cellulose, with the already mentioned properties.

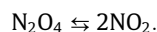
As an alternative to the present use of traditional halogenated solvents in the cellulose oxidation process [4–6], supercritical carbon dioxide (scCO₂) has been shown to be an attractive solvent to perform this oxidation [2]. Its major advantage in this case lies in its complete inertness regarding the oxidant, so, preventing a possible degradation of the solvent. Moreover, it ensures the biocompatibility of the processed material, because the latter is free from any solvent residue. Finally, because nitrogen dioxide is soluble in high pressure CO₂, it allows operation with a significant concentration of this reactant in the solvent. In a previous paper [2], efficiency of the cellulose oxidation was shown to depend on operating parameters such as pressure, temperature, moisture content, and CO₂ vs NO₂ ratio. Moreover, in this process, the knowledge of the number of phases and their composition is also a key parameter to obtain an oxidized product with tightly specified properties and for the development of the process on an industrial scale.

In the oxidation process, the reacting mixture, composed of the oxidant NO₂ and the solvent CO₂, is characterized by the existence

* Corresponding author at: INP-ENSIACET, 4 Allée Emile Monso, BP 44362, F-31030 Toulouse cedex 4, France. Tel.: +33 534323713; fax: +33 534323690.

E-mail address: severine.camy@ensiacet.fr (S. Camy).

of a chemical equilibrium between nitrogen dioxide and its dimer, nitrogen tetroxide (N_2O_4), as follows:



Below $T = 262.15$ K, the mixture is completely dimerised (N_2O_4), and this dimer dissociates as temperature increases, the proportion of each compound depending on conditions of temperature and pressure, the equilibrium being governed by the mass action law, with an equilibrium constant K depending only on the temperature. Under atmospheric pressure, the mixture boils at $T = 294.25$ K, the liquid being yellowish brown and the vapour reddish brown. If moisture is present, the mixture decomposes readily into nitrous and nitric acid, and becomes very aggressive to numerous metals.

Physical properties of the $\text{NO}_2/\text{N}_2\text{O}_4$ system, and values of the equilibrium constant, with respect to the temperature, have been the subject of several experimental and theoretical studies. For example, Reamer and Sage [7] have performed density measurements in the liquid–vapour coexistence region. Values of equilibrium constants in the vapour phase as a function of temperature can be found in works by Verhoek and Daniels [8] or Chao *et al.* [9]. These results describe a vapour phase containing mostly dissociated NO_2 (around 90 mol% of NO_2 at $T = 373.15$ K and a complete dissociation at 413.15 K). James and Marshall [10] have measured equilibrium constants in liquid phase and have shown that nitrogen dioxide is strongly associated in that physical state. Redmond and Wayland [11] have measured equilibrium constant data for nitrogen dioxide dissolved in some organic solvents.

Some authors studied the reaction of oxidation with NO_2 of cellulose in different organic solvents [12] and showed that the degree of dissociation of NO_2 increases in non-polar solvents, leading to an increase in the degree of oxidation of cellulose. So, although it is not yet clearly demonstrated, it is very probable that only the NO_2 molecule, *i.e.*, the monomer form, is the active oxidant molecule. Therefore, knowledge of the distribution between monomeric and dimeric species, especially when the oxidant NO_2 is solubilized in a solvent, appears to be an important parameter of the reaction.

This work reports experimental data of high-pressure equilibrium between CO_2 and NO_2 in conditions close to operating conditions of the cellulose oxidation process, which have already been described in the literature [2]. As a result of a collaborative study, an attempt to model the thermodynamic behaviour of this mixture has been published by Belkadi *et al.* [13], who used the crossover soft-SAFT equation of state to predict (vapour + liquid) equilibrium of this mixture under pressure. The soft-SAFT equation of state is a modification of the original Statistical Associating Fluid Theory (SAFT) molecular-based equation of state, which is in nature able to describe the thermodynamic behaviour of associating compounds [14]. Belkadi *et al.* have shown that predictions matched correctly experimental data of the ($\text{CO}_2 + \text{NO}_2/\text{N}_2\text{O}_4$) mixture provided that a binary interaction coefficient fits the experimental results. Although this kind of equation of state is a powerful tool to predict the thermodynamic behaviour of such a system, soft-SAFT equation is not implemented in most commercial thermodynamics software, and thus, from now, they cannot be easily used to compute fluid phase equilibrium of this mixture. Similarly, Bourasseau *et al.* [15] used the experimental results described in the present study, to show that (vapour + liquid) equilibria of the ($\text{CO}_2 + \text{NO}_2/\text{N}_2\text{O}_4$) mixture could be predicted using a Monte-Carlo molecular simulation approach. Their interest in this mixture is justified by the necessity to predict atmospheric ($\text{CO}_2 + \text{contaminants}$) mixtures. Interestingly, their simulations at $T = 300$ K predict a very low amount of non associated NO_2 molecules in both phases, but they could not compare this result with experimental ones. However, Monte-Carlo simulation is not a common tool that can be routinely used to predict fluid phase equilibria.

In this paper, the experimental set-up and conditions in which (vapour + liquid) equilibria and volumetric properties of the ($\text{CO}_2 + \text{NO}_2/\text{N}_2\text{O}_4$) mixture have been obtained will be described, and an attempt will be made to describe a way to predict the experimental data of this mixture using the well-known Peng–Robinson equation of state, in order to use this model in the specific context of the industrial application of cellulose oxidation.

2. Experimental

2.1. Materials

Liquid NO_2 (water content max 0.5 wt.%) and high purity CO_2 TP (N45 mass fraction purity 0.99999) were supplied by Air Liquide.

2.2. Specific hazards due to nitrogen dioxide handling

Nitrogen dioxide is a non-flammable and highly toxic gas (deadly poison). By consequence, a threshold limit value of $9 \cdot 10^{-6}$ by volume, *i.e.*, $9 \text{ mg} \cdot \text{m}^{-3}$, is recommended as the maximum concentration allowable in industrial premises [16]. For the purpose of this study, operators are protected thanks to a polypropylene transparent barrier guard placed around the experimental set-up, and an efficient ventilation of the whole set-up is ensured. Individual protection equipments are used too.

Before starting experiments, the entire installation must be carefully dried in order to remove moisture, as any trace of water would lead to HNO_3 formation and therefore metal corrosion. Moreover, every gasket of the installation must be made of Teflon[®] because NO_2 tends to soften most polymeric matter.

It should be pointed out here that in spite of corrosion protections, the experimental campaign has unfortunately been prematurely interrupted because of frequent NO_2 leaks occurring in pump or tubing of the system. These technical problems explain the limited number of experimental points that have been obtained.

2.3. High-pressure equipment

The experimental set-up is a SITEC (SITEC-Sieber Engineering AG, Switzerland) high pressure phase equilibrium apparatus. The complete set-up is presented in figure 1. This high-pressure unit allows detection and measurement of phase equilibrium and phase transitions by optical and analytical means. It is composed of a variable volume view cell (from 46.1 cm^3 to 60.2 cm^3) equipped with sapphire windows, a magnetic stirrer and a circulation pump for a better homogenization of the system. Sampling of gaseous and liquid phases can be taken from the top and the bottom of the cell, in which case the directly connected counterbalance piston operates to keep the pressure in the cell constant. The temperature of the cell is maintained by a thermostated bath. Measurement of temperature is taken by a thermocouple (J type, precision ± 0.1 K) placed in the centre of the cell. Phase transitions can be directly observed through sapphire windows, or filmed and transmitted by a connected camera, and displayed on a video screen.

Pressure inside the cell is measured by a pressure sensor (Keller) with accuracy of ± 0.075 MPa.

Data of the process throughout (pressure, temperature, position of the piston) are recorded on a computer.

Both fluids (CO_2 and $\text{N}_2\text{O}_4/\text{NO}_2$) are stored inside bottles at their (liquid + vapour) equilibrium at ambient temperature. So, the pressure of CO_2 inside the bottle is around (5 to 6) MPa, while pressure inside the NO_2 bottle is around 0.1 MPa. A correlation from DIPPR[®] database giving the NO_2 vapour pressure is presented in figure 2.

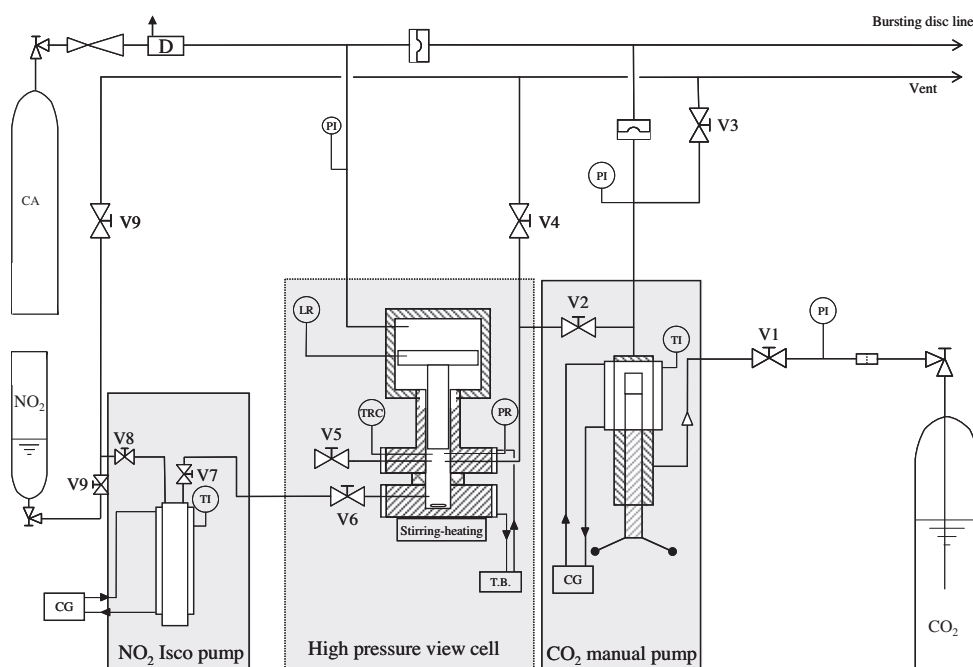


FIGURE 1. High-pressure phase equilibrium equipment (CA: compressed air; CG: cooling group).

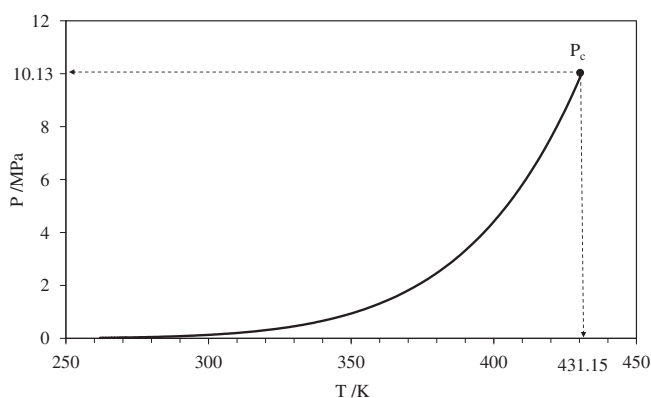


FIGURE 2. Vapour pressure of NO_2 as a function of temperature ($\ln P = 42.779 - 4431.7/T - 2.997 \ln T + 9.7289e^{-6} \cdot T^2$, $T = [261.9 - 431.15]$ K, P in MPa).

Carbon dioxide is introduced into the cell by action of a high pressure manual piston pump. This pump is cooled by a circulation of cold water in an external jacket, and pressure inside the pump is measured with a manometer. The amount of CO_2 that is introduced into the equilibrium cell is calculated through measurement of the difference between the volume of liquid CO_2 inside the manual pump, before and after its introduction.

Because of the very high toxicity of NO_2 , introduction of this compound into the equilibrium cell cannot be made as usually, *i.e.* by depositing the liquid or the solid in the open cell before closing and introducing of CO_2 . Rather, the procedure of introduction of this compound is similar to that of CO_2 , *i.e.* NO_2 is injected into the CO_2 pressurized cell, using a thermostated ISCO pump (Teledyne, model 260D).

2.4. Experimental procedure

Before starting an experiment, the whole system is flushed with gaseous CO_2 in order to remove any trace of water in the system. Then, the desired amount of carbon dioxide is introduced into

the cell with the CO_2 manual pump. The manual pump is first filled with liquid CO_2 and the temperature and pressure of the system are allowed to establish themselves. Introduction of CO_2 is made by opening valve V2. The volume of the manual pump is then adjusted in order to reach previous conditions of pressure and temperature of CO_2 (*i.e.* initial conditions before introduction). The difference in volumes inside the manual pump allows calculation of the mass of CO_2 introduced into the cell, with knowledge of the density of liquid CO_2 at temperature and pressure of the manual pump.

The procedure of introducing the NO_2 is similar to the CO_2 one, *i.e.* amount of NO_2 introduced into the cell is known by measurement of volume of NO_2 introduced, directly given by ISCO pump. The corresponding mass of NO_2 introduced into the cell is deduced through calculation (see section 3.1) of the density of NO_2 at temperature and pressure of ISCO pump.

Amounts of CO_2 and NO_2 introduced into the equilibrium cell are estimated and then chosen in order that a phase transition can be observed, when moving the piston inside the cell before reaching its maximum range. After introduction, the cell is pressurized with the piston in such a way that the mixture becomes a single phase one. The system is maintained in that position for several hours, until no change in temperature or pressure is observed. After this equilibration time, the cell is very carefully depressurized by retracting the piston. Special care is necessary in order to maintain a constant temperature inside the cell during this depressurization step. This point is very delicate because depressurization of the mixture induces sharp changes in temperature of the system. So, the depressurization is slowly operated until phase transition is observed. Temperature, pressure and piston position are recorded by computer during the operation. Pressurization–depressurization steps are repeated twice in order to check repeatability of the method.

When phase transition from a single phase to a two-phase system occurs, a sharp change in the moving speed of the piston is observed. Indeed, at equilibrium pressure, where a liquid and a vapour phases are present, the piston rises completely, changing vaporization ratio of the system without any pressure change. This

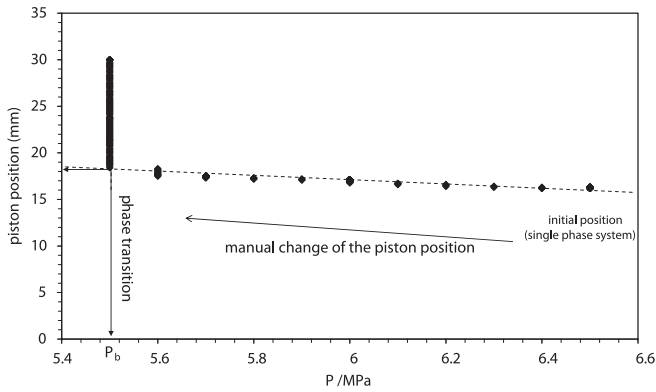


FIGURE 3. Example of pressure and piston position recording along an experiment.

appears very clearly when pressure and piston position are recorded as can be seen for example in figure 3. From this recording, the volume of the liquid phase at the pressure transition can be calculated and thus, knowing the amounts of introduced CO_2 and NO_2 , density of the liquid phase can be calculated.

3. Results

3.1. Evaluation of measurement uncertainties

The experimental set-up previously described allows determination of transition pressure, *i.e.* bubble or dew pressure, for a fixed composition and temperature of the mixture. This is a very specific system and it has been found useful to assess the composition, pressure and temperature uncertainties associated with such experimental devices.

Measurements are taken after isothermal conditions have been reached, temperature being measured by a thermocouple whose accuracy is ± 0.1 K.

In a first approach, evaluation of the uncertainty of the transition pressure measurements appears rather difficult because estimation of the phase transition point is partly subjective, its occurrence being visually decided by the operator. This drawback is nevertheless counterbalanced by the use of the recorded curves of the change in pressure, temperature, and position of the piston of the cell throughout the experiment. Indeed, phase transition corresponds to a sharp change in compressibility, and thus, around this boundary region the change in pressure presents a stiffness (figure 3). With this procedure, the phase transition pressure from a one-phase to a two phase mixture can objectively be determined and the pressure uncertainty can be directly related to the precision of the pressure sensor, *i.e.* ± 0.075 MPa in the case of this study.

Uncertainty of the mixture mass fraction can be calculated from conventional error calculation, starting from the expression of the mass fraction of one of the two compounds:

$$x_1 = \frac{V_1 \cdot \rho_1}{V_1 \cdot \rho_1 + V_2 \cdot \rho_2}, \quad (1)$$

V_i and ρ_i being respectively the volume and density of the compound i .

The absolute deviation of x_1 has been deduced by the differentiation of the expression (1).

The piston displacement of the manual syringe pump containing the liquid CO_2 gives the liquid CO_2 volume introduced into the measurement cell. The accuracy of this measurement is $\pm 1 \text{ cm}^3$. Volume of NO_2 introduced is directly obtained from the ISCO pump with a precision of $\pm 1 \cdot 10^{-3} \text{ cm}^3$.

Liquid CO_2 density is calculated using the Lee, Kesler and Plöcker (LKP) equation of state [17], giving a very satisfying correspondence with the experimental density values from Ely *et al.* [18] over a wide range of temperature and pressure, as shown in figure 4.

The LKP calculations are performed using Simulis® Thermodynamics, a commercial thermophysical properties server – PROSIM S.A. (France). It allows thermodynamic properties and equilibrium calculations for pure component and mixture fluid phase. Density estimation was obtained with mean error of $\pm 6.2 \text{ kg} \cdot \text{m}^{-3}$, when compared to the experimental results of Ely *et al.*, who estimated the uncertainty of their measured densities to be equal to 0.02%.

In a similar way, $\text{NO}_2/\text{N}_2\text{O}_4$ liquid density uncertainty has been estimated by comparing calculations with experimental data from the literature [7]. These experimental results give the temperature dependence of the density of the saturated liquid of the $\text{NO}_2/\text{N}_2\text{O}_4$ system. The Rackett's equation [19] has been used to estimate the liquid density of $\text{NO}_2/\text{N}_2\text{O}_4$, using Simulis® Thermodynamics. This model used with the DIPPR® data for $\text{NO}_2/\text{N}_2\text{O}_4$ fits the experimental values, as shown in figure 5. Mean error of NO_2 density prediction ($\Delta\rho_{\text{NO}_2}$) is equal to $\pm 8.5 \text{ kg} \cdot \text{m}^{-3}$.

In the same way, uncertainties of mixture liquid density measurements have been evaluated. Density of the liquid mixture is calculated by measuring position of the piston of the equilibrium cell when phase transition occurs (equation (2)). Thus, it is obtained by dividing total mass of the mixture (m_{mix}) introduced into the cell by the volume of the liquid phase (V_L), this latter being calculated with the minimum volume of the cell (bottom position of

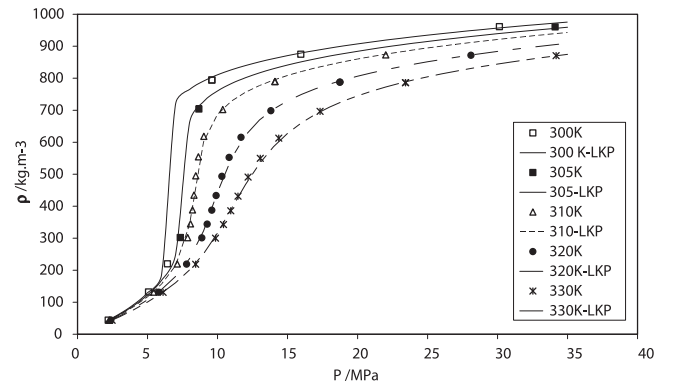


FIGURE 4. Comparison of experimental [16] and LKP calculated values of CO_2 density (mean error $6.2 \text{ kg} \cdot \text{m}^{-3}$).

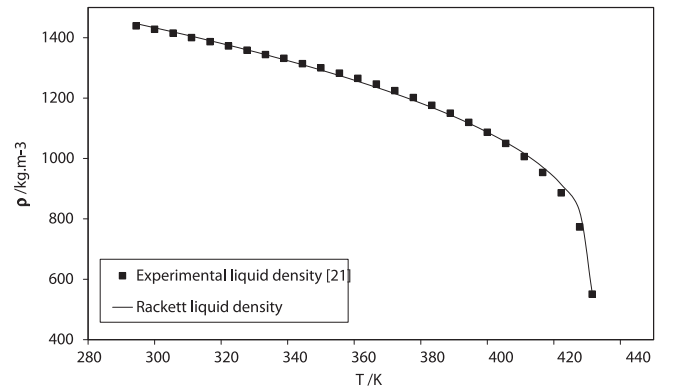


FIGURE 5. Temperature dependence of liquid density of $\text{NO}_2/\text{N}_2\text{O}_4$ system at (vapour + liquid) equilibrium. Comparison of experimental [7] and calculated values with the Rackett's equation (mean error $8.5 \text{ kg} \cdot \text{m}^{-3}$).

TABLE 1

Evaluated uncertainties.

Measured parameter	Evaluated uncertainty
T/K	0.1
P/MPa	0.075
$\Delta V_{\text{CO}_2}/\text{cm}^3$	1
$\Delta V_{\text{NO}_2}/\text{cm}^3$	$1 \cdot 10^{-3}$
$\Delta \rho_{\text{CO}_2}/\text{kg} \cdot \text{m}^{-3}$	6.2
$\Delta \rho_{\text{NO}_2}/\text{kg} \cdot \text{m}^{-3}$	8.5
$\Delta V_0/\text{cm}^3$	0.5
$\Delta h_{\text{piston}}/\text{mm}$	0.1

the piston) (V_0) and with the measured position of the piston at phase transition (h_{piston})

$$\rho_L^{\text{mix}} = \frac{m^{\text{mix}}}{V_L} = \frac{m_{\text{CO}_2} + m_{\text{NO}_2}}{V_0 + \pi \cdot \frac{d_{\text{piston}}^2}{4} \cdot h_{\text{piston}}} = \frac{V_{\text{CO}_2} \cdot \rho_{\text{CO}_2} + V_{\text{NO}_2} \cdot \rho_{\text{NO}_2}}{V_0 + \pi \cdot \frac{d_{\text{piston}}^2}{4} \cdot h_{\text{piston}}} \quad (2)$$

The V_{CO_2} and V_{NO_2} are the volumes of liquid CO_2 and $\text{NO}_2/\text{N}_2\text{O}_4$ introduced into the cell and ρ_{CO_2} and ρ_{NO_2} are their densities calculated at the temperature and pressure of each pump.

Again, the absolute deviation in the liquid phase density has been deduced by the differentiation of the expression (2).

Measurements uncertainties ΔV_{CO_2} , ΔV_{NO_2} , $\Delta \rho_{\text{CO}_2}$, and $\Delta \rho_{\text{NO}_2}$ have been evaluated as described above. Volume of the cell V_0 has been measured to an accuracy of $\pm 0.5 \text{ cm}^3$ and the piston position is measured to an accuracy of $\pm 0.1 \text{ mm}$.

Finally, measurements uncertainties are presented in table 1.

3.2. Experimental P - x data and liquid densities of $(\text{CO}_2 + \text{NO}_2/\text{N}_2\text{O}_4)$ mixture at high pressure

The experimental set-up described in the previous section does not allow measuring the degree of dissociation of N_2O_4 inside the equilibrium cell, only the overall mass of $\text{NO}_2/\text{N}_2\text{O}_4$ mixture introduced into the cell is measured. So, it has been decided initially to appoint the $\text{NO}_2/\text{N}_2\text{O}_4$ mixture as an apparent pure NO_2 compound (termed “app NO_2 ” in this work). The ternary ($\text{CO}_2 + \text{NO}_2 + \text{N}_2\text{O}_4$) system is thus fictively considered as a binary ($\text{CO}_2 + \text{appNO}_2$) system.

Although the equilibrium cell is supposed to allow dew-points measurements (transitions from one vapour phase to a two phase system), this type of experiment is actually very tricky because the

formation of the first liquid droplet is really difficult to observe in the cell. As a consequence, in this work, experimental data mainly concern bubble pressures.

Experimental results and their related measurement uncertainties are presented in table 2.

As explained earlier, for safety reasons, the number of experiments has been quite low. However, the findings are sufficient to yield a good estimation of behaviour of the mixture, at temperature corresponding to operating conditions of cellulose oxidation conditions.

4. Modelling and discussion

The NO_2 and N_2O_4 form a reacting binary system with only one degree of freedom at (liquid + vapour) equilibrium. That is why in the (P, T, x) coordinates, the two-phase region of this reacting system is a curve which ends at the critical point of these molecules. Thus, the critical coordinates T_c , P_c and the acentric factor ω are the same for NO_2 and N_2O_4 . The fugacities calculated with a cubic equation of state are the same for NO_2 and N_2O_4 too. To calculate the equilibrium of such a ternary system, the only equation where NO_2 and N_2O_4 are distinguishable is the chemical equilibrium between NO_2 and N_2O_4 , where the standard Gibbs free energies and enthalpies of formation get involved. In a first approach, the case of the hypothetical binary ($\text{CO}_2 + \text{appNO}_2$) mixture without considering NO_2 - N_2O_4 chemical equilibrium was considered. Calculations of fluid-phase equilibrium of this pseudo-binary mixture, obtained from a conventional equation of state have been compared to experimental results. Calculations have been performed with Simulis® Thermodynamics. Because ($\text{CO}_2 + \text{appNO}_2$) mixture involves apolar compounds, the well-known Peng–Robinson (PR) cubic equation of state [20] was chosen to describe the thermodynamic behaviour of the mixture.

In the case of a mixture, parameters a , α and b of PR equation of state are calculated using a mixing rule, involving the attraction term a_i , the co-volume b_i , and α_i parameters of pure components. Standard van der Waals mixing rules involving mixture composition z_i , with one binary interaction coefficient for parameter a , have been chosen here in this work. Critical parameters and acentric factor of pure compounds necessary for calculations are gathered in table 3.

Conventional mixing rules bring into play one binary interaction parameter k_{ij} , to take account of the specific interactions exist-

TABLE 2Transition pressures (P) and liquid density measurements of different $(\text{CO}_2 + \text{appNO}_2)$ mixtures at different temperatures. Compositions are expressed in mass fractions.

T/K	x_{CO_2}	x_{appNO_2}	P/MPa	Δx_{CO_2}	Type	$\rho_L/\text{kg} \cdot \text{m}^{-3}$	$\Delta \rho_L/\rho_L \cdot 100$
298.15	0.072	0.928	1.000	0.014	Bubble	n.m. ^a	
313.65	0.281	0.719	3.300	0.013	Bubble	1338.3	3.20
312.95	0.323	0.678	3.800	0.012	Bubble	1255.9	2.99
313.05	0.355	0.645	4.200	0.011	Bubble	1195.4	2.83
313.05	0.937	0.063	8.000	0.003	Bubble	551.1	5.44
313.35	0.778	0.222	6.620	0.006	Bubble	1152.9	3.47
313.35	0.784	0.216	6.690	0.006	Bubble	1229.9	3.47
313.55	0.788	0.212	6.770	0.006	Bubble	1171.1	3.37
313.35	0.546	0.455	5.550	0.011	Bubble	1172.6	3.58
313.35	0.571	0.430	5.500	0.010	Bubble	1196.8	3.45
313.35	0.586	0.414	5.520	0.010	Bubble	1158.0	3.32
313.25	0.606	0.394	5.600	0.009	Bubble	1144.0	3.17
313.15	0.136	0.864	2.100	0.014	Bubble	1384.4	3.13
313.65	0.160	0.840	2.560	0.013	Bubble	1329.2	3.02
312.35	0.884	0.116	5.500	0.010	Dew	n.m.	
328.45	0.839	0.161	8.970	0.007	Bubble	950.7	3.29
328.45	0.847	0.153	8.950	0.007	Bubble	873.8	3.10
328.45	0.707	0.293	7.810	0.010	Bubble	n.m.	

^a Not measured.

TABLE 3

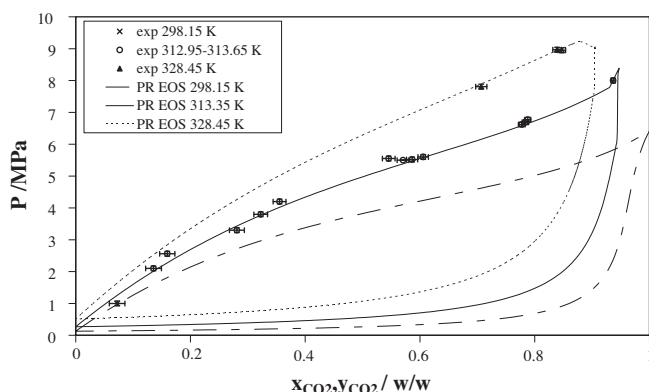
Parameters of pure compounds (from DiPPr database).

	T_c/K	P_c/MPa	ω
CO ₂	304.15	7.37600	0.231
NO ₂	431.15	10.13252	0.851088
N ₂ O ₄	431.15	10.13252	0.851088

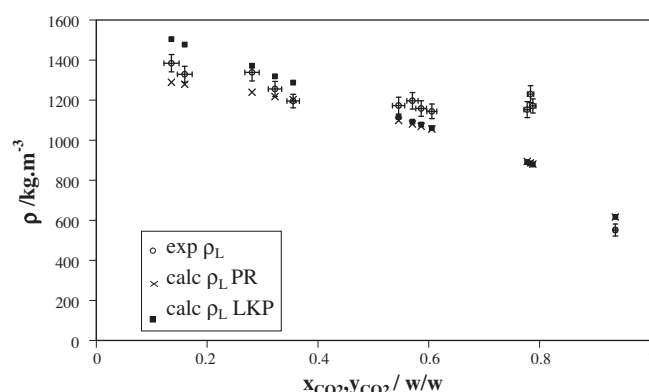
ing between components in the mixture. This parameter is usually obtained by matching experimental data with the equation of state.

In the case of (CO₂ + appNO₂) mixture, it can be seen from figure 6 that PR EoS predict reliable values of bubble pressure even using $k_{ij} = 0$. Experimental results are plotted with experimental errors given in table 1. These values of $k_{ij} = 0$ mean that no specific interactions between CO₂ and appNO₂ exist in fluid phases.

In the same way, volumetric behaviour of the saturated liquid phase (at bubble point) of the (CO₂ + appNO₂) mixture has been evaluated using the PR EoS. Although it is well known that cubic equations of state derived from van der Waals theory are not very suitable to calculate liquid molar volumes, PR EoS is considered to give a better restitution of this property. Liquid density has been also evaluated with the LKP equation of state. For both calculations,

**FIGURE 6.** Comparison of experimental and calculated (P, x, y) data for the (CO₂ + appNO₂) system.**TABLE 4**Experimental and calculated liquid density of different (CO₂ + appNO₂) mixtures at different temperatures. Compositions are expressed in mass fractions.

Experimental results					PR calculations			LKP calculations	
T/K	x_{CO_2}	x_{appNO_2}	P_b/MPa	$\rho_L/(kg \cdot m^{-3})$	$\rho_L/(kg \cdot m^{-3})$	Relative deviation/%		$\rho_L/(kg \cdot m^{-3})$	Relative deviation/%
298.15	0.072	0.928	1.000	n.m.	1350.99	n.c. ^a		1636.07	n.c.
313.65	0.281	0.719	3.300	1338.3	1239.65	7.96		1371.56	2.43
312.95	0.323	0.678	3.800	1255.9	1217.67	3.14		1318.42	4.74
313.05	0.355	0.645	4.200	1195.4	1202.88	0.63		1287.44	7.15
313.05	0.937	0.063	8.000	551.1	616.21	10.56		616.21	10.56
313.35	0.778	0.222	6.620	1152.9	893.95	28.97		890.88	29.41
313.35	0.784	0.216	6.690	1229.9	886.93	38.66		884.27	39.08
313.55	0.788	0.212	6.770	1171.1	880.79	32.96		878.42	33.32
313.35	0.546	0.455	5.550	1172.6	1098.06	6.79		1115.04	5.16
313.35	0.571	0.430	5.500	1196.8	1080.42	10.77		1092.06	9.59
313.35	0.586	0.414	5.520	1158.0	1068.99	8.33		1077.60	7.46
313.25	0.606	0.394	5.600	1144.0	1055.39	8.40		1060.62	7.86
313.15	0.136	0.864	2.100	1384.4	1288.75	7.42		1504.47	7.98
313.65	0.160	0.840	2.560	1329.2	1279.25	3.90		1477.01	10.01
328.45	0.884	0.116	8.970	950.7	651.77	45.87		651.77	45.87
328.45	0.839	0.161	8.950	873.8	648.69	34.70		458.18	90.71
328.45	0.847	0.153	7.810	n.m.	875.15	n.c.		867.50	n.c.

^a Not calculated.**FIGURE 7.** Experimental (°) and calculated with PR EoS (x) and LKP EoS (■) saturated liquid density for the (CO₂ + appNO₂) system at temperatures between 312.95 K and 313.65 K.

liquid density is calculated at experimental temperature, bubble pressure and mass composition of the (CO₂ + appNO₂) mixtures.

Experimental and calculated results are given in table 4. For a clearer visualization of the results, experimental and calculated densities at temperature around 313.15 K are presented in figure 7.

From figure 7, a sharp discrepancy between experimental and calculated results for mixtures such that x_{CO_2} is around 0.8 is observed, whatever the model. From table 4, this can also be observed for high temperature measurements. Results for $x_{CO_2} \approx 0.8$ are quite surprising when compared to others, so an experimental artefact may be suspected for these results. Overall, our experimental results are roughly predicted by these EOS, PR EoS giving slightly better results but the precision remains poor.

However, it is not surprising that the volumetric behaviour of the liquid phase cannot be well predicted without taking into account the equilibrium between N₂O₄ and NO₂ inside the mixture. Indeed, density of the mixture is highly dependent on the real composition of the mixture, i.e. proportion of NO₂ and N₂O₄ in the presence of CO₂. Moreover, our results do not enable us to deduce proportion of each compound by fitting experimental results with PR EoS since the parameters of pure compounds involved in the EoS are the same for NO₂ and N₂O₄ (T_c , P_c , and ω).

5. Conclusions

This work has provided experimental data about the high pressure ($\text{CO}_2 + \text{NO}_2/\text{N}_2\text{O}_4$) phase equilibria. Although this first approach for modelling the liquid–vapour experimental study did not allow a complete description of the actual behaviour of the system, *i.e.*, the dissociation degree of N_2O_4 was not measured and modelled, the modelling, using a simple Peng–Robinson equation of state with $k_{ij} = 0$ was shown, nevertheless, to be very suitable for predicting the physical state of the ($\text{CO}_2 + \text{NO}_2/\text{N}_2\text{O}_4$) mixture, within the given range of pressure and temperature which is of interest for the targeted process of oxidation of cellulose. Therefore, it achieves one of its objectives, *i.e.*, providing a simple tool to predict the phase diagram in the reactor and to determine the maximum amount of NO_2 which can be dissolved in CO_2 as the solvent to maintain a single-phase oxidant fluid medium in the solid–fluid reactor. Having this knowledge is essential for the future development of the new process of oxidation of cellulose.

References

[1] E.J. Beckman, J. Supercrit. Fluids 28 (2004) 121–191.

[2] S. Camy, S. Montanari, A. Rattaz, M. Vignon, J.S. Condoret, J. Supercrit. Fluids 51 (2009) 188–196.
[3] M. Vignon, S. Montanari, D. Samain, J.S. Condoret, WO 2006/018552, 2006.
[4] W.O. Kenyon, E.C. Yackel, US 2 448 892, 1948.
[5] W.H. Ashton, C.E. Moser, US 3 364 200, 1968.
[6] F. Boardman, L. Saferstein, EP 0 492 990 A1, 1991.
[7] H.H. Reamer, B.H. Sage, Ind. Eng. Chem. 44 (1952) 185–187.
[8] F.H. Verhoek, F. Daniels, J. Am. Chem. Soc. 53 (1931) 1250–1263.
[9] J. Chao, R.C. Wilhoit, B.J. Zwolinski, Thermochim. Acta 10 (1974) 359–371.
[10] D.W. James, R.C. Marshall, J. Phys. Chem. 72 (1968) 2963–2966.
[11] T.F. Redmond, B.B. Wayland, J. Phys. Chem. 72 (1968) 1626–1629.
[12] M.M. Pavlyuchenko, F.N. Kaputskii, D.D. Grinshpan, Zh. Prikl. Khim. 48 (1975) 1822–1825.
[13] A. Belkadi, F. Lovell, V. Gerbaud, L.F. Vega, Fluid Phase Equilib. 266 (2008) 154–163.
[14] F.J. Blas, L.F. Vega, Mol. Phys. 92 (1997) 135–150.
[15] E. Bourasseau, V. Lachet, N. Desbiens, J.-B. Maillet, J.-M. Teuler, P. Ungerer, J. Phys. Chem. B 112 (2008) 15783–15792.
[16] <http://www.cdc.gov/niosh/npg/npgd0454.html>.
[17] U. Plockner, H. Knapp, J. Prausnitz, Ind. Eng. Chem. Process. Des. Dev. 17 (1978) 324–332.
[18] J.F. Ely, W.N. Haynes, B.C. Bain, J. Chem. Thermodyn. 21 (1989) 879–894.
[19] R.D. Gunn, T. Yamada, AIChE J. 18 (1973) 234.
[20] D.-Y. Peng, D.B. Robinson, Ind. Eng. Chem. Fundam. 15 (1976) 59–64.